Theor Appl Climatol
DOI 10.1007/s00704-013-1056-0

ORIGINAL PAPER

Simulating the influence of the South Atlantic dipole on the South Atlantic convergence zone during neutral ENSO

Rodrigo J. Bombardi · Leila M. V. Carvalho · Charles Jones

Received: 15 July 2013 / Accepted: 26 November 2013

Abstract The South Atlantic Convergence Zone (SACZ) is an intrinsic characteristic of the South American Summer Monsoon. In a recent study, we verified that the main mode of coupled variability over the South Atlantic (South Atlantic Dipole (SAD)) plays a role in modulating the position of extratropical cyclones that affect the SACZ precipitation. In this study, we perform numerical experiments to further investigate the mechanisms between SAD and the SACZ. Numerical experiments forced with prescribed SST anomalies showed that, even though the Atlantic SST affects the position of the cyclone associated with the SACZ, the atmospheric response and precipitation patterns over land are opposed to the observations. On the other hand, experiments forced with prescribed anomalous driving fields showed that the atmospheric component of SAD plays a significant role for the right position and intensity of precipitation associated with the SACZ. SAD negative anomalies provide the low-level and upper-level atmospheric support for the intensification of the cyclone at surface and for the increase in precipitation over the land portion of the SACZ. Therefore, the numerical experiments suggest that, during El Niño Southern Oscillation neutral conditions, the SACZ precipitation variability associated with SAD is largely dependent on the atmospheric variability rather than the underlying SST.

1 Introduction

The South Atlantic Convergence Zone (SACZ) is a prominent feature of the South American Monsoon (Zhou and Lau 1998), characterized by a quasistationary baroclinic zone oriented in the northwest–southeast direction that extends from the Amazon to the subtropical South Atlantic Ocean (Carvalho LM et al. 2004; Carvalho LM et al. 2002b; Kodama 1993; Kodama 1992; Liebmann et al. 2001). The quasistationary baroclinic zone is supported by a low-level convergence of moisture and by an upper-level subtropical jet. There are two major moisture flows converging into the SACZ: One is associated with the circulation of the South Atlantic subtropical high and the other flows eastward from the South American monsoon region along the SACZ (Kodama 1992, 1993). The monsoon heat source plays two roles in maintaining the SACZ. One is by inducing the summertime strengthening of the South Atlantic subtropical high (Rodwell and Hoskins 2001) and consequently forming a low-level flow along the eastern periphery of the thermal low toward the subtropics. The other is by generating a strong subtropical jet in the southern flank of the upper-level anticyclone (Kodama 1999).

Active SACZ periods are characterized by the presence of anomalous low-level westerly flow over tropical Brazil, with convergence of moisture over central and southeastern Brazil. Likewise, inactive SACZ is associated with anomalous low-level easterly flow over tropical Brazil (Carvalho et al. 2002a; Herdies 2002; Jones and Carvalho 2002). The anomalous westerly winds transport air with high moist static energy from the Amazon into the SACZ region, favoring deep convection (Chou and Neelin 2001). Most of the extreme events of precipitation over southeastern Brazil, during the austral summer, are associated with the intensification of the SACZ (Carvalho et al. 2002b).

Previous studies (e.g., Bombardi et al. 2013; Robertson and Mechoso 2000) have shown evidence that the dominant mode of coupled variability over the South Atlantic Ocean, known as the "South Atlantic Dipole" (henceforth SAD) plays an important role for the variability of the SACZ on intraseasonal to interannual time scales. SAD is characterized by a dipole in

R. J. Bombardi (✉) · L. M. V. Carvalho · C. Jones
Department of Geography, University of California, Santa Barbara, Santa Barbara, CA 93106-3060, USA
e-mail: rbombard@gmu.edu

Published online: 15 December 2013

sea surface temperature anomalies (Fig. 1) with centers over the tropical and the extratropical South Atlantic (Nnamchi et al. 2011; Sterl and Hazeleger 2003; Venegas et al. 1997). The dominant variability of SAD is observed on interdecadal timescales (Venegas et al. 1997). However, SAD also shows significant variability on intraseasonal timescales (Bombardi et al. 2013; Bombardi and Carvalho 2011).

SAD mechanisms are related to the strengthening and weakening of the South Atlantic subtropical anticyclone, with the atmosphere leading the ocean by 1–2 months (Venegas et al. 1997). During the strengthening of the subtropical anticyclone, there is an intensification of the wind stress in the tropical Atlantic that increases evaporation, enhances the ocean's surface loss of latent heat, and increases the depth of the ocean's mixed layer. A deeper mixed layer is less susceptible to the heating by shortwave radiation leading to negative SST anomalies in the tropics (Morioka et al. 2011). During the decay phase of SAD, the SST anomalies are damped by entrainment and latent heat flux, suggesting that SST changes do not feedback on the atmospheric circulation in a systematic way between the onset and the demise of SAD (Morioka et al. 2011; Sterl and Hazeleger 2003). Although the dominant variability is generated by internal atmospheric dynamics, SAD is still significantly affected by SST variability (Haarsma et al. 2005).

Observational studies have shown significant evidence of a relationship between the SAD SST patterns and precipitation over the SACZ region. Robertson and Mechoso (2000) verified that, on interannual timescales, intense SACZ events were associated with cold SST anomalies in the tropical Atlantic and warm SST anomalies in the extratropical South Atlantic. Extreme wet events over southeastern Brazil are related to negative SST anomalies over the tropical South Atlantic and positive SST anomalies over the subtropical South Atlantic (Muza et al. 2009). In addition, temperatures over southeastern Brazil are also correlated with SAD (de O Cardoso and Silva Dias 2004). Negative SST anomalies over the tropics and positive SST anomalies over the extratropics are related to increased precipitation during the rainy season over eastern Brazil (Bombardi and Carvalho 2011). Moreover, Bombardi et al. (2013) observed that SAD events are associated with changes in the position of generation and trajectories of extratropical cyclones. As a consequence, changes in the cyclones' track affect convection over the SACZ region.

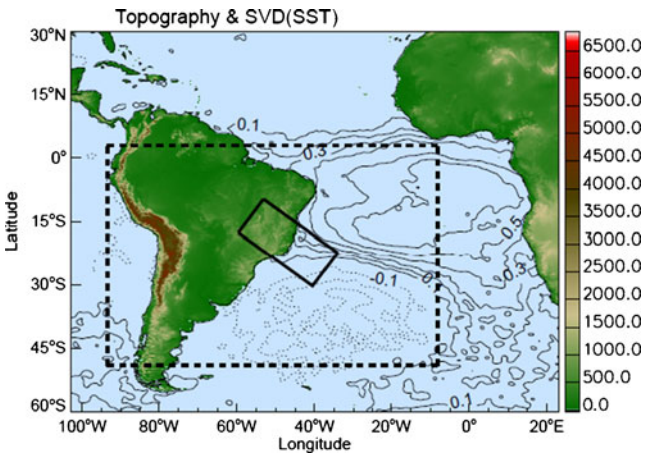

Fig. 1 Topography (*shaded*) and correlation between the SAD index (as defined in (Bombardi et al. 2013) and SST (contour). *Solid lines* present positive correlation and *dotted lines* present negative correlation. The *dashed box* shows the domain of the regional atmospheric simulations and the *solid line* box represents the region of interest under the influence of the SACZ (see text for details)

Interestingly, experiments with global atmospheric models perturbed with SAD spatial pattern of SST anomalies seem to simulate variations in the SACZ that contradict observational studies (e.g., Haarsma 2003; Robertson et al. 2003). Robertson et al. (2003) performed experiments with an atmospheric global circulation model (UCLA-AGCM) with prescribed SST anomalies in the boundary conditions. They verified that the SST dipole pattern observed by Robertson and Mechoso (2000) does not significantly influence the simulated SACZ and associated circulation and precipitation anomalies. Haarsma (2003) performed simulations with a general circulation model (SPEEDY) forced with prescribed positive SST anomalies in the tropics and negative SST anomalies in the extratropics. They observed a southward shift of the Inter-Tropical Convergence Zone with increased precipitation over northeast Brazil, consistent with some observational results (e.g., Bombardi and Carvalho 2011; Moura and Shukla 1981; Uvo et al. 1998). However, they also verified an increase in precipitation over the oceanic SACZ region, which contradicts observational results (e.g., Bombardi and Carvalho 2011; Robertson and Mechoso 2000). In addition, precipitation anomalies in the experiments of Haarsma (2003) and Robertson et al. (2003) were largely confined to the ocean.

The goal of this study is to further investigate the mechanisms relating SAD atmospheric and oceanic perturbations to variations in the SACZ precipitation by performing regional atmospheric simulations. The numerical experiments were designed to investigate the relative importance of SST anomalies (surface boundary conditions) and atmospheric driving fields (initial and lateral boundary conditions) during SAD events and their impact on the SACZ precipitation. More specifically, the objective of these simulations is to investigate the SAD's influence on the location and strength of the cyclone associated with the SACZ and, consequently, its influence on convection and circulation along the convergence zone. Two sets of experiments were performed: (1) perturbed SST conditions (experiments using perturbed surface boundary conditions) and (2) perturbed driving fields (experiments using perturbed initial and lateral boundary conditions). The focus of this study is on a SACZ event that occurred between December 11 and 16 of 2005. This event was particularly interesting as the SACZ developed during neutral El Niño

Southern Oscillation (ENSO) and neutral SAD conditions. This study is organized as follows: "Section 2" introduces the regional model used in this study and the dataset used to integrate and to validate the simulations. The control experiment is discussed in "Section 3." "Section 4" shows the results from SST sensitivity experiments. "Section 5" shows the results from experiments with perturbed atmospheric driving fields. The conclusions are presented in "Section 6."

2 Regional atmospheric model

The regional atmospheric simulations were performed using the Brazilian developments on the Regional Atmospheric Modeling System (RAMS; Pielke et al. 1992; Cotton et al. 2003). The purpose of this joint project (referred to as BRAMS) is to develop a regional model tailored to tropical conditions. BRAMS has been widely used for studies related to atmospheric chemistry and transport in Brazil (e.g., Alonso et al. 2010; Freitas et al. 2009; Longo et al. 2010). Recently, Santos et al. (2013) evaluated the performance of the simulation of daily precipitation by BRAMS during summer over Brazil using simple and weighted ensemble simulations. They found that a simple ensemble using different options of the convective parameterization scheme represents well the precipitation over southeastern Brazil. We used the BRAMS version 4.2, which is derived from the RAMS version 5.04. BRAMS is a non-hydrostatic model with several components to represent cloud microphysics processes, radiative transfer, turbulence, and atmosphere–biophysics–hydrology interactions. The atmosphere–biophysics–hydrology interactions are represented by the LEAF-2 (Land Ecosystem-Atmosphere Feedback) model (Walko et al. 2000). The LEAF-2 model represents the exchange of energy and moisture between the atmosphere and soil, vegetation, canopy air, temporary surface water, and permanent water bodies. The energy and moisture fluxes are divided into water transfer, heat transfer (by turbulent exchange, conduction, or precipitation), and long-wave radiative transfer. More information about BRAMS can be found at http://brams.cptec.inpe.br/).

2.1 Configuration

The experiments were performed with a single domain with 32 km spatial grid resolution. The 32 km spatial resolution was used by Tomaziello and Gandu (2013) with good results. The area of interest is the region under the influence of the SACZ shown by the northwest–southeast-oriented rectangle extending from southeastern Brazil toward the western South Atlantic Ocean (Fig. 1). This area encompasses the region with maximum signal of SAD over the continent (Bombardi et al. 2013) and also exhibits maximum variance in the outgoing long-wave radiation during summer in association with the SACZ (e.g., Carvalho et al. 2002b). The model top was set to about 22 km with top boundary nudging above 16 km. Lateral boundary nudging was used to keep the simulation evolving correctly in the context of observed large-scale flow field. However, model interior nudging is a severe constraint on the model simulation and significantly impacts the mesoscale circulations (Weaver 2002). Therefore, no interior model nudging was applied in this study. We used the Grell cumulus parameterization (Grell 1993) with Arakawa-Schubert closure (Arakawa and Schubert 1974) and the Chen-Cotton shortwave and long-wave radiation models (Chen and Cotton 1983). Table 1 summarizes the main information about the configuration of BRAMS.

2.2 BRAMS input data

Initial and lateral boundary conditions were obtained from the Modern Era Retrospective-Analysis for Research and Applications (MERRA) reanalysis, at 1.25° latitude×1.25° longitude grid spacing (Rienecker et al. 2011) and updated every 3 h. We used 37 vertical levels ranging from 1,000 to 0.1 hPa.

The vegetation type dataset was based on the MODIS normalized difference vegetation index. This dataset was created by the Terrestrial Biophysics and Remote Sensing Lab (http://tbrs.arizona.edu/cdrom/Index.html) on monthly temporal resolution and 30 s global spatial resolution. The soil texture was set to constant sandy clay loam. We used the constant sandy clay loam based on the experience of modelers in Brazil and personal communication with Dr. Edmilson Dias de Freitas. Dr. Freitas has performed several experiments with BRAMS and found out that the model's files for soil classes were not very accurate, and the model would perform better if the soil type was kept homogeneous and set to sandy clay loam. According to Dr. Freitas, sandy clay loam is the soil class available in BRAMS that best represents the dominant soil type of the region of interest, eastern Brazil. The land use and topography were provided by the United States Geological Survey at 1 km global spatial resolution. Soil moisture was initialized with the soil moisture data from the BRAMS group (Gevaerd and Freitas 2006). The soil moisture has eight soil layers, and it is estimated based on precipitation estimates from satellite data. More information can be found at http://brams.cptec.inpe.br/in_data_soil_moisture.shtml. All the input files for vegetation type, soil texture, soil moisture, land use, and topography are provided by the BRAMS group.

The SST data used were the NOAA Optimum Interpolation 0.25° daily Sea Surface Temperature Analysis (Reynolds et al. 2007). This dataset is based on satellite measurements (Advanced Very High Resolution Radiometer (AVHRR)) and in situ data from ships and buoys. The dataset is available from 1982 to the present. Tomaziello and Gandu (2013) investigated two SACZ events and verified that the skill of BAMS slightly improved when forced with the NOAA Optimum

Table 1 Summary of BRAMS configuration

Horizontal spatial resolution	32 km
Number of grid points in longitude	300
Number of grid points in latitude	240
Number of vertical levels	34
Model top	22 km
Lateral boundary region nudging	Yes (comprising five grid points on each lateral boundary). The nudging is performed every 1,800 s.
Top region nudging	Yes (all fields above 16 km; ~150 hPa)
Model interior nudging	No
Cumulus parameterization	Grell (Grell 1993)
Closure type	Arakawa-Schubert (Arakawa and Schubert 1974)
Shallow cumulus parameterization	Not used
Shortwave and long-wave radiation models	Chen-Cotton (Chen and Cotton 1983)

Interpolation 0.25° daily in comparison with the NOAA 1° resolution SST (Reynolds et al. 2002).

2.3 Precipitation data

To validate the skill of BRAMS in simulating the SACZ, we compared the precipitation simulated by BRAMS with the following daily precipitation datasets: Tropical Rainfall Measuring Mission (TRMM 3B42 V6); the Climate Prediction Center morphing method (CMORPH); the National Oceanic and Atmospheric Administration (NOAA) Climate Prediction Center (CPC) unified gauge precipitation (CPC-uni); and Brazilian National Agency of Waters (*Agencia Nacional das Aguas* (ANA)) gauge precipitation.

The TRMM Multisatellite Precipitation Analysis (Huffman et al. 2007) is based on precipitation estimates derived from passive microwave data collected by a variety of low earth orbit satellites and infrared data collected by the geosynchronous earth orbit satellites. The TRMM_3B42 V6 gridded rainfall algorithm uses an optimal combination of TRMM2B31 and TRMM2A12 data products, Special Sensor Microwave Imager (SSM/I), Advanced Microwave Scanning Radiometer (AMSR), and Advanced Microwave Sounding Units (AMSI) (Kummerow et al. 1998, 2000). This 3-hourly dataset was processed at daily resolution and 0.25° grid spacing and is described in Bookhagen and Strecker (2010).

The CMORPH precipitation analysis (Joyce et al. 2004) is derived from a technique that estimates precipitation from low orbiter passive microwave satellite scans and uses geostationary satellite infrared data information to propagate the precipitation by motion vectors. The precipitation data are available at high temporal and spatial resolutions from December 2002 to the present.

The CPC precipitation is based on an optimal interpolation technique to create gridded precipitation from station records (Chen et al. 2008; Higgins et al. 2000). The gridded precipitation is created at 0.5×0.5° grid spacing. A thorough discussion on the performance of CPC and TRMM_3B42 V6 in simulating the precipitation characteristics during the wet season in South America is provided in Carvalho et al. (2012).

The ANA precipitation dataset was interpolated into the same grid spacing as the BRAMS simulations (32 km) using ordinary kriging. Ordinary kriging is an interpolation technique that takes into account not only the values of the available records but also their spatial distribution (Marsal 1987). The technique was applied to the daily station records for the period of December 2005.

3 Control experiment

As discussed in the "Introduction," the SACZ event investigated here developed in December 2005 under atmospheric conditions characterized as neutral ENSO and neutral SAD. The SACZ exhibited a life cycle of about 6 days (December 11–16) which corresponds approximately to the 75th percentile of persistence of strong SACZ events identified in Carvalho LM et al. (2004)). The control experiment started on December 6 (5 days prior to the beginning of the SACZ event) and ended on December 20 (4 days after the end of the SACZ event) of 2005. Therefore, we allowed 5 days of model spin-up as recommended by Giorgi and Bi (2000). The atmospheric driving fields from MERRA were updated every 3 h and the soil moisture every 24 h. The SST used in the control experiment was the climatology of December from 1982 to 2009.

To obtain an estimate for the uncertainty of the modeling system, we performed ten-member ensemble simulations. The differences among ensemble members arise from small random perturbations in the boundary conditions. The perturbations were defined as 5 % of the standard deviation of the December climatology for each of the five variables that comprise the driving fields of the model. The random

perturbations were included in the boundary conditions for all five variables at all times except in the initial conditions. Hence, all ensemble members share the same initial conditions. As mentioned before, the top boundary nudging was set above 16 km to all fields (around 150 hPa). Therefore, in order to avoid performing nudging of perturbed fields at the top of the model, the anomalies were included in the vertical fields from the surface up to 200 hPa.

Figure 2 shows the evolution of the low-level winds and precipitation in the control experiments. On December 11 (Fig. 2a), a narrow band with significant precipitation and low-level wind convergence was simulated over eastern

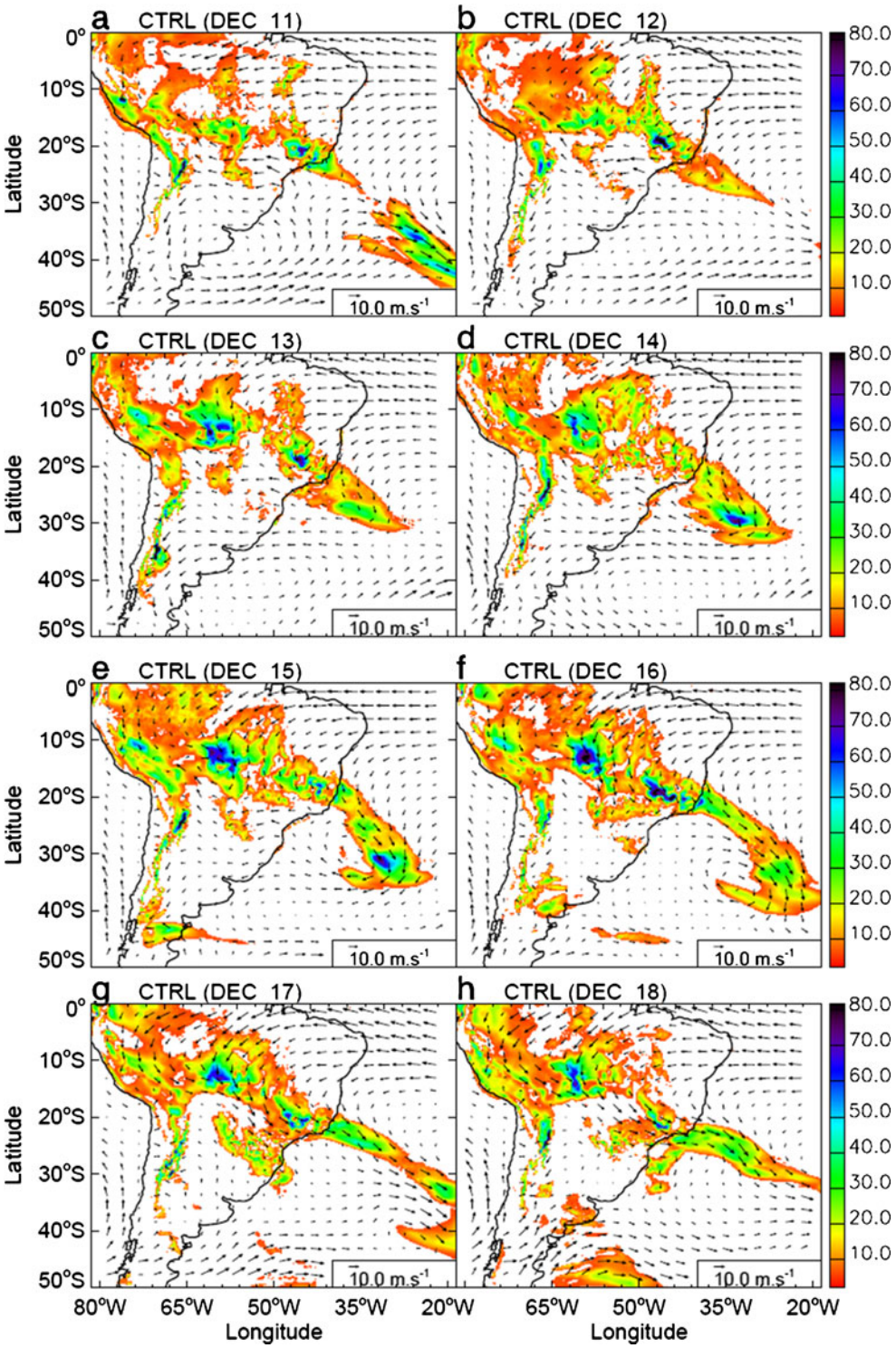

Fig. 2 Daily evolution of the control ensemble mean wind at 850 hPa (vectors) and the ensemble mean precipitation (*shaded*)

tropical South America and western Subtropical Atlantic, which characterized the presence of the SACZ. In addition, the 850 hPa circulation indicated the presence of a high pressure system in the southern flank of the SACZ over subtropical South America. Anticyclonic circulation and suppressed convective activity over southern Brazil, Uruguay, and Northeastern Argentina were realistic features and characterized the well-documented seesaw in convection and precipitation during SACZ events (e.g., Carvalho et al. 2004; Liebmann et al. 1999; Vera et al. 2006). Moreover, enhanced precipitation in the SACZ was simulated along with westerly winds associated with moisture transport from the Amazon, consistent with previous observational studies (Carvalho et al. 2004; Jones and Carvalho 2002; Rickenbach 2002). A low-level trough associated with the SACZ is simulated over Subtropical Atlantic east of 35°W. In the following days the simulated precipitation in the SACZ intensified over coastal areas as the high pressure system weakened and moved eastward (Fig. 2b–c). On December 14 (Fig. 2d), the simulations generate a well-defined cyclone system near the southeast coast of Brazil. In the next days (Fig. 2e–h), that cyclone migrated southeastward and the westerly winds intensified along a well-organized SACZ.

To evaluate the representation of precipitation in the control experiment, we focused our analyses on the region represented by the solid box in Fig. 1. The land and the ocean portions of that region were considered separately. Figure 3 shows the daily median precipitation from observations and simulations over land and over the ocean. Over the ocean, the model overestimated precipitation, especially on day 18 after the end of the SACZ event. However, the intensity of the simulated precipitation seems to be, to some extent, systematically higher than the intensity of the observed precipitation from TRMM and CMORPH (Fig. 3b). It is worth mentioning that TRMM precipitation estimates over the ocean are less reliable than estimates over land due to fewer in situ observations (Huffman et al. 2007). Nonetheless, Tomaziello and Gandu (2013) verified that BRAMS 4.2 has higher skill in representing the SACZ precipitation over land than over the ocean. In addition, we recall that the control experiment was performed with climatological SST, which could have played a role for the model's performance in simulating precipitation over the ocean. The following analyses focus on days 11 to 17 when the simulations showed the best performances.

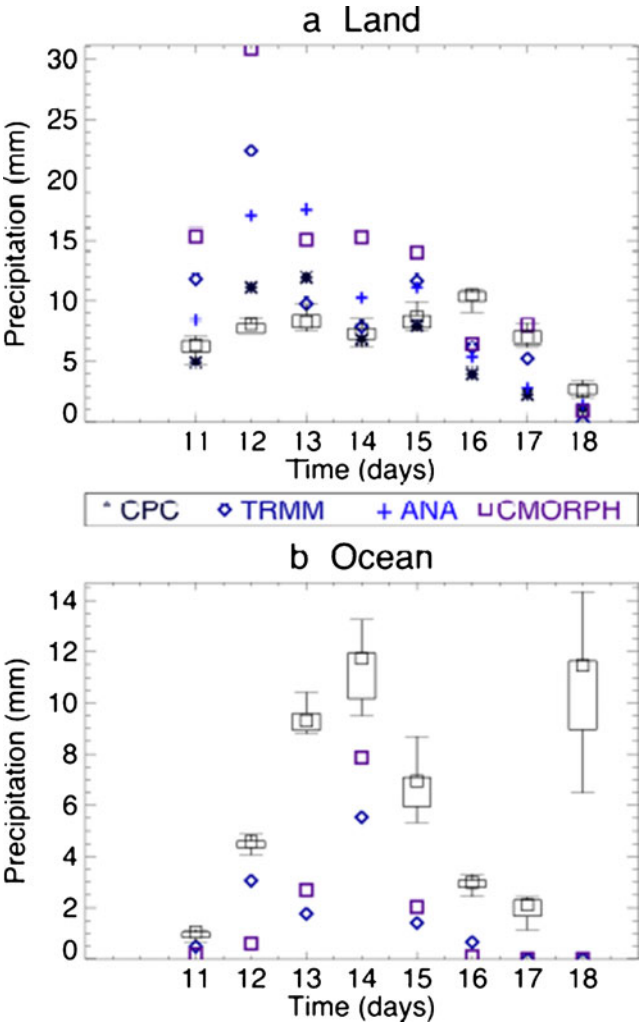

Fig. 3 Box plot of daily median ensemble precipitation (*square symbol*) for the control simulations (December 11–18) and daily precipitation from observations over **a** land and **b** the ocean. Precipitation from CPC and ANA are not available over the ocean. The box plot is built on the daily median precipitation of each ensemble member. The *whiskers* are defined as 1.5 times the interquartile range

4 SST sensitivity experiments

The SST sensitivity experiments were designed such that we use the same configuration as the control experiments but with modified SST conditions. In these experiments, the SST was the climatology from December plus prescribed anomalies. The spatial pattern and magnitude of the SST anomalies were based on composite analyses of the SAD index discussed in Bombardi et al. (2013) (see their Fig. 4a, b). Anomalies are included only over the Atlantic Ocean. We defined SAD-negative phase as the configuration characterized by negative SST anomalies in the tropics and positive SST anomalies in the extratropics. It is worth mentioning that what we call SAD negative phase is equivalent to the Positive South Atlantic Subtropical Dipole (Positive SASD) defined by Morioka et al. (2011).

In addition, instead of performing ensembles by adding random perturbations to the boundary conditions, we performed many simulations with different intensity of SST anomalies. The simulations were performed with 0.5, 1.0, 2.0, and 3.0 times the magnitude of the SST anomaly composites for both phases of SAD. For SAD negative phase, the experiments were called 0.5NEG, NEG, 2NEG, and 3NEG,

respectively. Likewise, for SAD positive phase, the experiments were called 0.5POS, POS, 2POS, and 3POS, respectively. Since we did not create ensembles for each SST simulation, we compared the results of the SST sensitivity experiment to a single member of the control experiment, the member that was not forced with random perturbations in lateral boundary conditions. Thus, the only differences among these simulations are the SST anomalies. The complete range of the ensemble CTRL runs will be explored in "Section 5."

The SST sensitivity experiments resulted in a change in the position of the SACZ (Fig. 4). Simulations with the negative SAD SST patterns shifted the position of the SACZ to the south of the domain, while simulations with the positive SAD SST patterns shifted the position of the SACZ to the north,

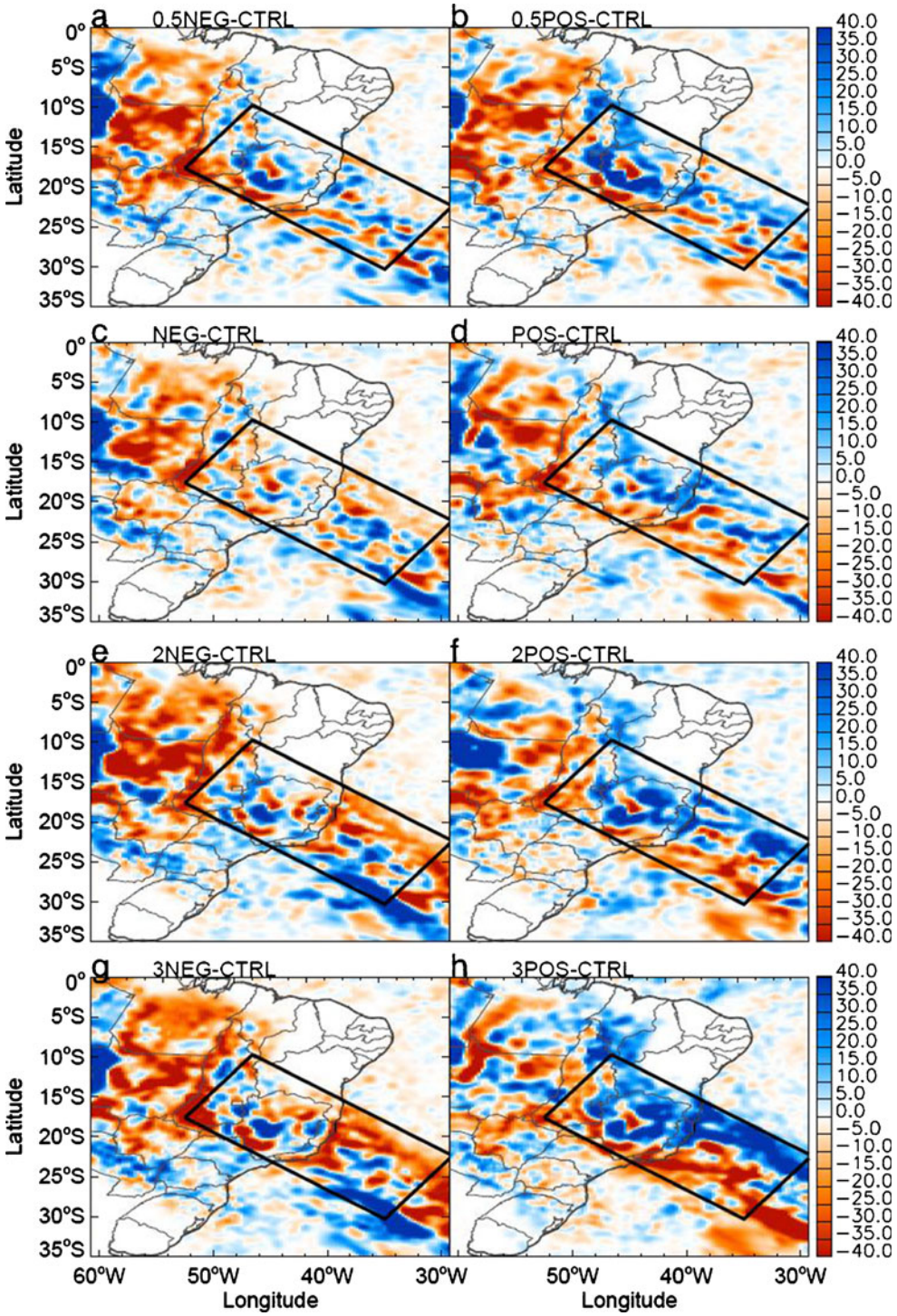

Fig. 4 Accumulated precipitation differences [millimeters] between each SST sensitivity simulation and the control simulation

with displacements depending on the intensity of the anomaly. This is particularly evident over the ocean and in the simulations with more extreme perturbations, which are two or three times the magnitude of the SST composites (Fig. 4e–h).

These results are consistent with numerical studies of the impact of the Atlantic Ocean SST on the SACZ on seasonal to interdecadal timescales (Barreiro et al. 2002; Chaves and Nobre 2004). Chaves and Nobre (2004) used atmospheric (CPTEC/COLA) and oceanic (GFDL MOM2) general circulation models to study the relationship between the tropical South Atlantic SST anomalies and the seasonal variability of the SACZ during the austral summer (November through February). They verified that warm SST anomalies over the tropical South Atlantic intensify and move the SACZ northward, while cold SST anomalies weaken this system over land and sea. Barreiro et al. (2002) performed simulations with the Community Climate Model (CCM3) forced with global observed SST. The authors found that the South Atlantic SST interannual-to-interdecadal variability impacts the SACZ precipitation over the ocean. They verified positive SST anomalies in the tropics and negative SST anomalies in the extratropics were associated with increased precipitation to the north of the oceanic position of the SACZ.

Interestingly, although the SST sensitivity experiments showed a change in the position of the SACZ, there was no clear change in the amount of accumulated precipitation over the continental SACZ region (Fig. 5a). This result is also in agreement with other numerical studies that verified a small influence of the South Atlantic SST on precipitation over South America (Barreiro 2009; Barreiro et al. 2002; Cuadra and Da Rocha 2007; Haarsma 2003; Robertson et al. 2003). Cuadra and Da Rocha (2007) examined the seasonal predictability of the Regional Climate Model version 3 (RegCM3; 50 km spatial resolution) by assuming persisted SST anomalies during the wet season. They verified that the interannual variability of the simulated seasonal rainfall and air temperature over South America were practically unaffected by prescribed SST. Barreiro (2009) used an atmospheric global circulation model coupled to a slab ocean in which the SST anomalies were generated only through changes in the fluxes of heat to the atmosphere. The author found that the South Atlantic did not directly influence the precipitation over subtropical South America on interannual timescales.

In addition, there was no systematic change in the amount of accumulated precipitation over the oceanic SACZ region in the SST sensitivity simulations (Fig. 5b). However, other numerical studies verified that the South Atlantic SST has a strong impact on precipitation over the oceanic portion of the SACZ (Barreiro 2009; Barreiro et al. 2002, 2005; Chaves and Nobre 2004; Cuadra and Da Rocha 2007; Haarsma 2003; Jorgetti 2008; Robertson et al. 2003; Taschetto and Wainer

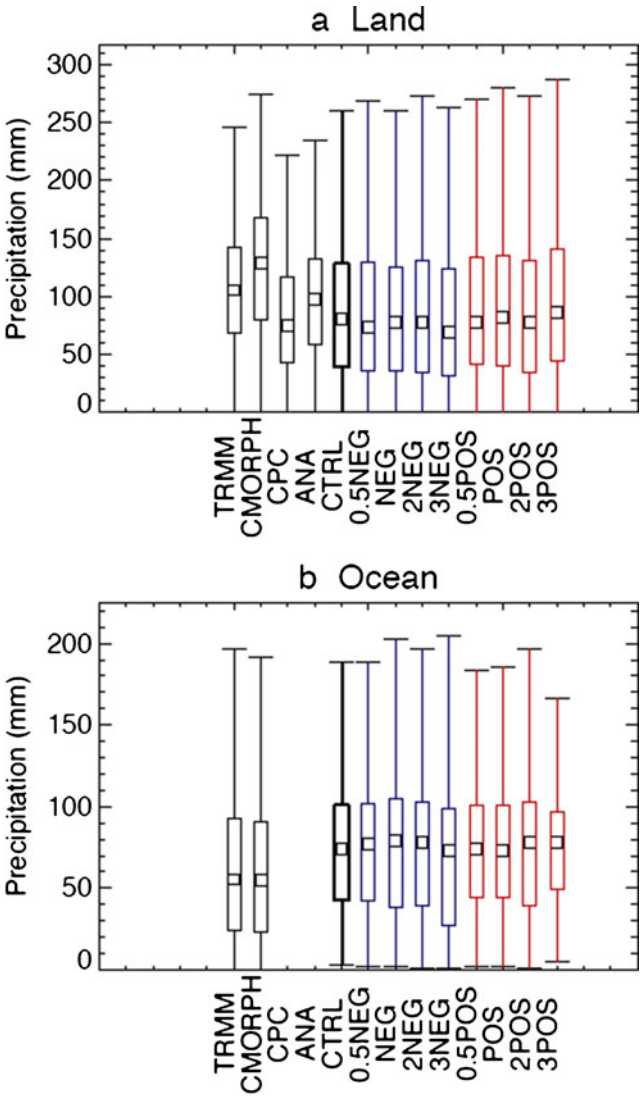

Fig. 5 Box plot of accumulated precipitation from December 11 to 17 over **a** land and **b** the ocean. The box plot is built on the spatial distribution of accumulated precipitation. The *whiskers* are defined as 1.5 times the interquartile range. Observations are shown in *black*; the control experiment is shown in *black* thick lines; SAD-negative simulations are shown in *blue*, and SAD-positive experiments are shown in *red*

2008). This discrepancy could be related to some extent to BRAMS 4.2 relatively poorer skill in simulating the SACZ over the ocean than over land (Tomaziello and Gandu 2013).

The observational analyses of Bombardi et al. (2013) indicated a relationship between SAD and the position and intensity of extratropical cyclones in the subtropical South Atlantic associated with the development of the SACZ. Here we examine these issues by investigating differences in SLP between the SST sensitivity and the control simulations. In the control simulation (i.e., with climatological SST), a cyclone forms near southeast Brazil between December 14 and 15 (Fig 6d, e) and then propagates southeastward (Fig. 6f–h). To evaluate the changes in the cyclone location among the SST sensitivity experiments, we tracked the position of the

cyclone from its formation (15Z December 14) until the cyclone approaches the boundary of the area of interest in our domain (21Z December 16). We stopped tracking the cyclone beyond that point to avoid analyzing results that might be influenced by lateral boundary conditions. The results clearly show that the warmer the tropical SST, the larger the northeastward displacement of the cyclone (Fig. 7). Likewise, the colder the tropical SST the larger the southwestward displacement of the cyclone (Fig. 7). However, the northeast–southwest displacement of the cyclone in SST sensitivity experiments is contrary to the observational studies (Bombardi et al. 2013), and this reversal occurs independently of the intensity of the SST anomalies.

We evaluated changes among SST sensitivity simulations by calculating the BIAS and the Root Mean Square Error (RMSE) between each member of the SST sensitivity experiment and the control run, based on the methodology used by Giorgi and Bi (2000). Although both quantities are measures of deviation, the RMSE measures the overall magnitude of deviations regardless of their individual signs, while the BIAS measures systematic or predominant deviations in given directions. The RMSE is calculated according to Eq. 1, where X_i^S is the "ith" variable of interest (SST sensitivity experiments), X_i^O the "ith" variable of reference (control experiment), and N is the number of points. The BIAS is calculated according to Eq. 2.

$$RMSE = \sqrt{\frac{1}{N}\sum_{i=1}^{N}\left(X_i^S - X_i^O\right)^2} \quad (1)$$

$$BIAS = \frac{1}{N}\sum_{i=1}^{N}\left(X_i^S - X_i^O\right) \quad (2)$$

Figure 8 shows the BIAS in latent (Fig. 8a) and sensible (Fig. 8b) heat fluxes following the cyclone. For each cyclone track of each SST sensitivity simulation, we calculated the BIAS spatially between that simulation and the control run, in a circular area of 1,000 km diameter. The objective of this analysis is to verify whether the surface fluxes resulting from the SST sensitivity runs play a role in the location of the cyclone. Notice that the circular area around the tracks of the cyclones simulated in each SST sensitivity run does not necessarily coincide with the area around the tracks of the cyclone simulated by the control run. We observe that positive SST anomalies in the tropics increase the latent and sensible heat fluxes to the atmosphere modifying the position of formation and the trajectory of the cyclone, which is displaced northward (Fig. 8). On the other hand, colder SST anomalies in the tropics and warm anomalies in the subtropics decrease the flux of latent and sensible heat to the atmosphere in the tropical South Atlantic favoring the formation and displacement of the cyclone further south.

Therefore, these experiments revealed that the position and trajectory (northeast–southwest displacement) of the cyclones and the SACZ in an atmosphere observed in ENSO neutral and SAD neutral conditions seem to depend essentially on where the warming is occurring over the ocean. That is, the sensible and heat fluxes to the atmosphere seem to be the main forcing for the SACZ and the associated cyclone. In the southern hemisphere, cold and dry air is advected to the west of the cyclone whereas warm moist air is advected to the east of the cyclone. The cold and dry air favors the intensification of heat fluxes from the ocean to the atmosphere whereas the warm and moist air reduces the heat fluxes (e.g., Reboita 2008). Hence, when the extratropics are colder than normal (POS), the colder and drier air moving into the cyclone region increases the heat fluxes behind the system. On the other hand, when the extratropics are warmer than normal (NEG), there is a reduction of the heat fluxes behind the system.

Although the SST sensitivity experiment shows that SAD SST pattern influences the location of cyclogenesis and the SACZ, the response in the numerical simulations contradicts the observational results from Bombardi et al. (2013). These results are consistent with Barreiro et al. (2002) and Robertson et al. (2003) and suggest that the SACZ precipitation variability associated with SAD is largely dependent on the atmospheric variability rather than the underlying SST. However, Barreiro (2009) indicates that wind stress and oceanic processes might also be important in determining the SST anomalies in the South Atlantic and consequently modifying the impact of the ocean in the atmosphere, which are exactly the mechanisms of SAD proposed by Morioka et al. (2011).

In reality, during a SAD event, the atmosphere and the ocean would evolve together. Therefore, the differences between observational and atmospheric modeling studies might be partially related to ocean–atmospheric feedbacks that cannot be represented in atmospheric models. Chaves and Nobre (2004) verified the occurrence of a negative ocean–atmosphere feedback in the SACZ region. Warm SST anomalies over the tropical South Atlantic tend to intensify and move the SACZ northward. As a consequence, the cloudiness associated with the SACZ blocks incoming solar radiation leading to a cooling of the region under the influence of the SACZ. On the other hand, cold SST anomalies tend to weaken the SACZ over land and sea, leading to a warming of the surface due to incoming solar radiation (Almeida et al. 2007; Chaves and Nobre 2004). Jorgetti (2008) performed case studies during active and inactive SACZ periods with BRAMS coupled and uncoupled to an oceanic mixed layer model and obtained results consistent with Chaves and Nobre (2004). The author suggests that the SST plays an important role in the correct

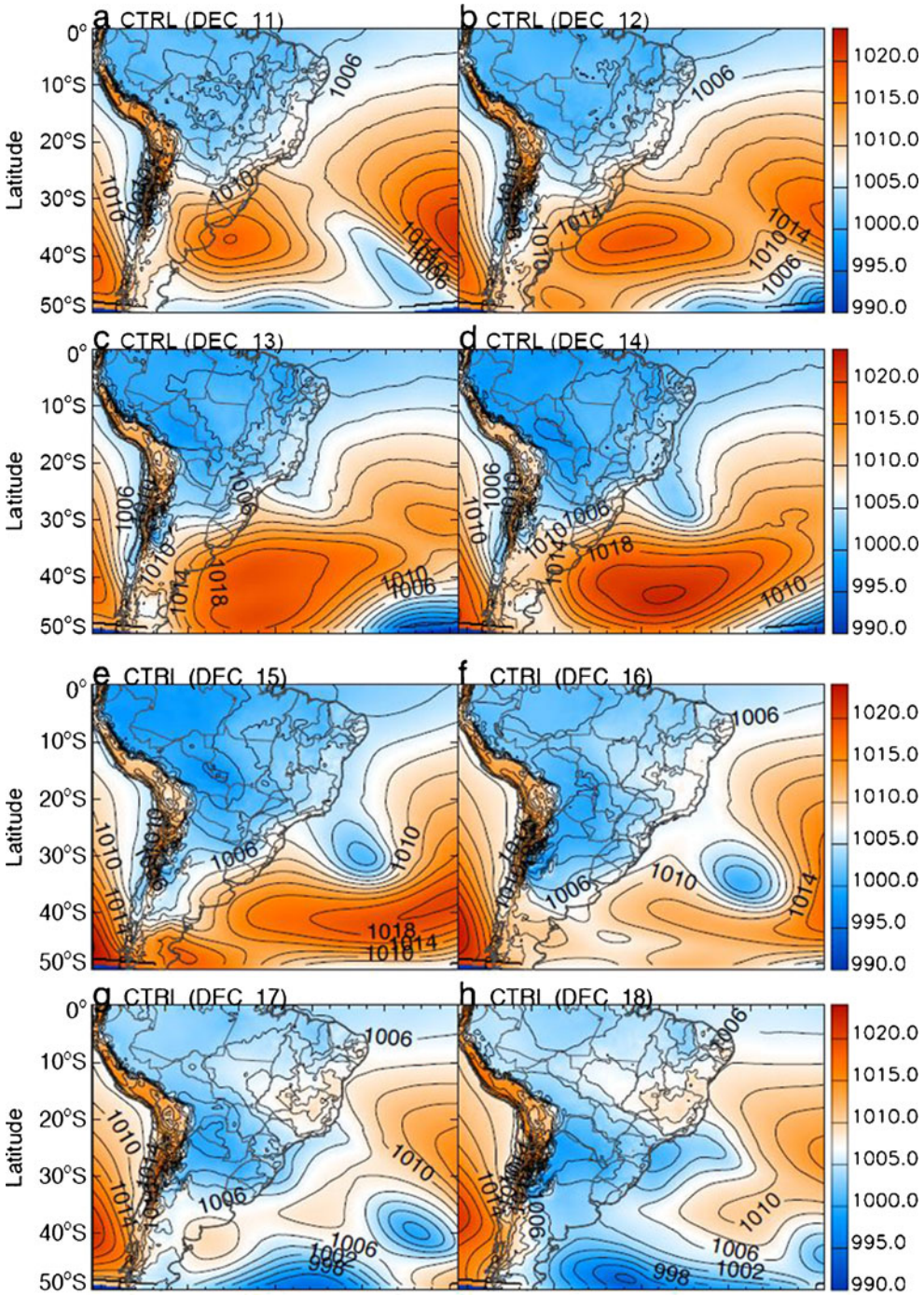

Fig. 6 Evolution of daily SLP in the control simulation

representation of moisture transport responsible for the generation and the maintenance of the SACZ. For active SACZ periods, the coupled experiments tend to reduce the SST underneath the SACZ cloud coverage in comparison to the uncoupled experiments, due to a reduction in the incoming solar radiation. As a consequence, there is a reduction in the convergence of moisture flux, leading to a reduction in the precipitation associated with the SACZ in the coupled experiment. Although much insight can be gained from coupling regional models, the relative importance of the atmospheric anomalous conditions during SAD in driving the observed variability of the SACZ has yet to be demonstrated. The next section investigates the relative importance of the atmospheric forcing during SAD events.

5 Driving field experiments

A new set of experiments was designed to investigate the importance of the atmospheric conditions during SAD events

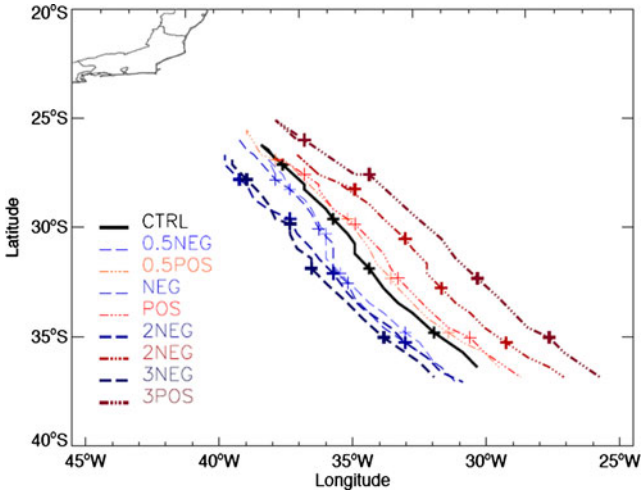

Fig. 7 Cyclone tracks for a member of the control experiment and the members of the SST sensitivity experiment. The symbol "x" represents the position of the cyclone for every 12 h starting at 00Z on December 15

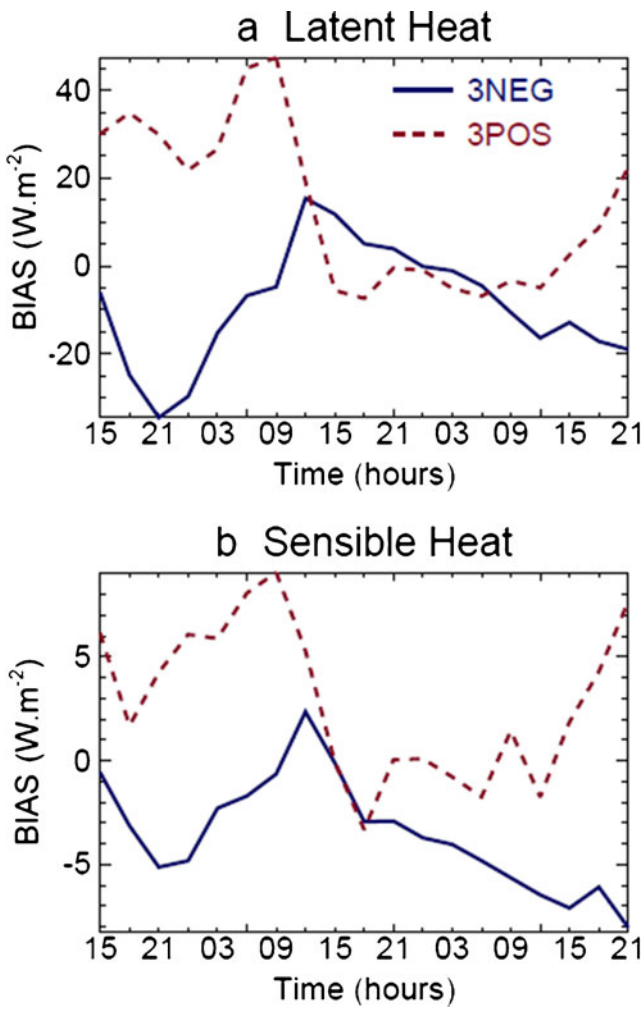

Fig. 8 **a** Latent heat BIAS and **b** sensible heat BIAS following the cyclone tracks of the simulations with three times the magnitude of SAD (3NEG and 3POS). The BIAS was calculated spatially for 3-hourly averages from 15Z December 14 to 21Z December 16. *Solid lines* indicate 3NEG and *dashed lines* 3POS experiments

for the position of the cyclone and organization of precipitation in the SACZ. In these experiments, BRAMS configuration was the same as the control experiments (Table 1). The model was forced with December climatological SST but with prescribed anomalies in the initial and boundary conditions of the atmospheric driving fields, which are zonal and meridional wind, temperature, geopotential height, and relative humidity. To maintain the balance between the atmospheric fields in the model, we included prescribed anomalies in all five driving fields. The methodology to select the spatial pattern and magnitude of the atmospheric perturbations was similar to the methodology used in Bombardi et al. (2013) to define SAD events. Taking the SAD time index obtained in Bombardi et al. (2013) (see their Fig. 3), we selected cases when the SAD phase was positive (above 75th percentile) or negative (below 25th percentile) during the month of December and during neutral ENSO periods. We recall that the SST spatial pattern of positive SAD phase as defined in this work is similar to Fig. 1 and is equivalent to the negative SASD convention used by Morioka et al. (2011). For each SAD phase, we performed composites of the following anomalous fields (annual cycle removed): horizontal wind, temperature, geopotential height, and relative humidity (BRAMS driving fields from MERRA Reanalysis) at all vertical levels. The prescribed atmospheric anomalies were then included in the initial condition fields and in the boundary conditions at all times for all five variables. The anomalies were included in the vertical fields from the surface up to 200 hPa. We also performed ensemble simulations using the same methodology applied to the control experiment (see "Section 3"). We performed a ten-member ensemble for each phase of SAD. We will refer to the SAD-negative phase simulations as "NEG" and to the SAD-positive phase simulations as "POS."

Figure 9 shows the difference in the ensemble median accumulated precipitation between the perturbed and the control experiments. The NEG experiments simulated increased precipitation over eastern South America and adjacent ocean (Fig. 9a). These simulations indicated that atmospheric conditions during the negative phase of SAD (i.e., negative SST anomalies over tropical South Atlantic), intensify and shift the SACZ position northward. On the other hand, the POS experiments (positive SST anomalies over tropical South Atlantic) simulated a weakening of the SACZ with decreased precipitation over eastern South America (Fig. 9b). These results are consistent with the observational analyses of Bombardi et al. (2013).

Figure 10 and Table 2 indicate changes in the distribution of the accumulated precipitation (millimeters per day) simulated in the control, POS, and NEG experiments over land and ocean (from December 11 to 17). The box plot of the accumulated precipitation was calculated taking into account all the members of each experiment (Fig. 10). Over land, the spatial distribution of the accumulated precipitation simulated

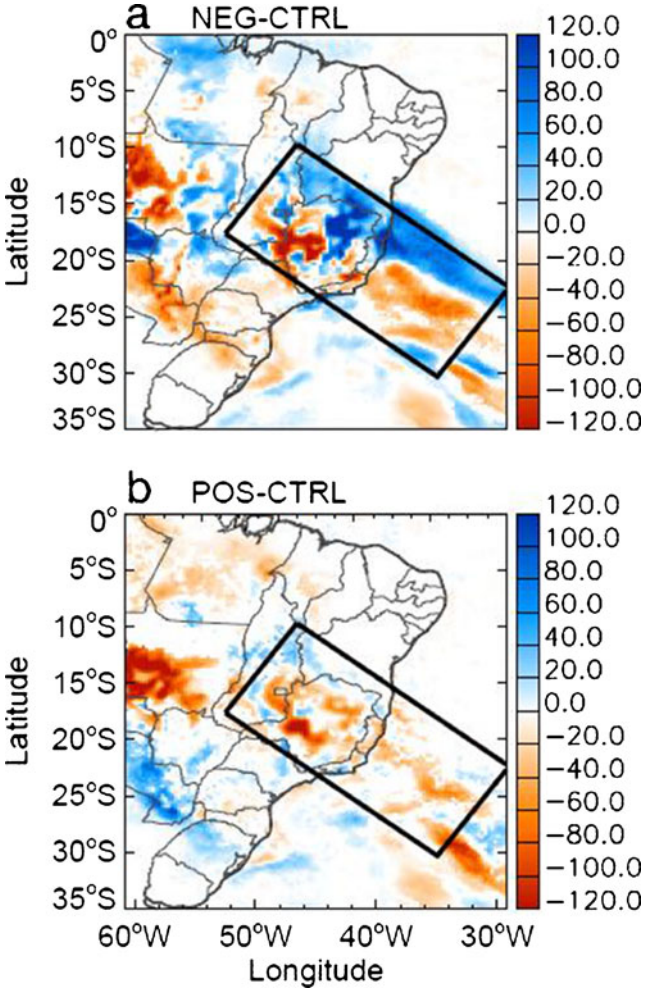

Fig. 9 Difference in the ensemble median accumulated precipitation from December 11 to 17 between **a** NEG and control experiments; **b** POS and control experiments. In the figure are displayed only ensemble median differences that are statistically significant at 5 % level according to the sign test

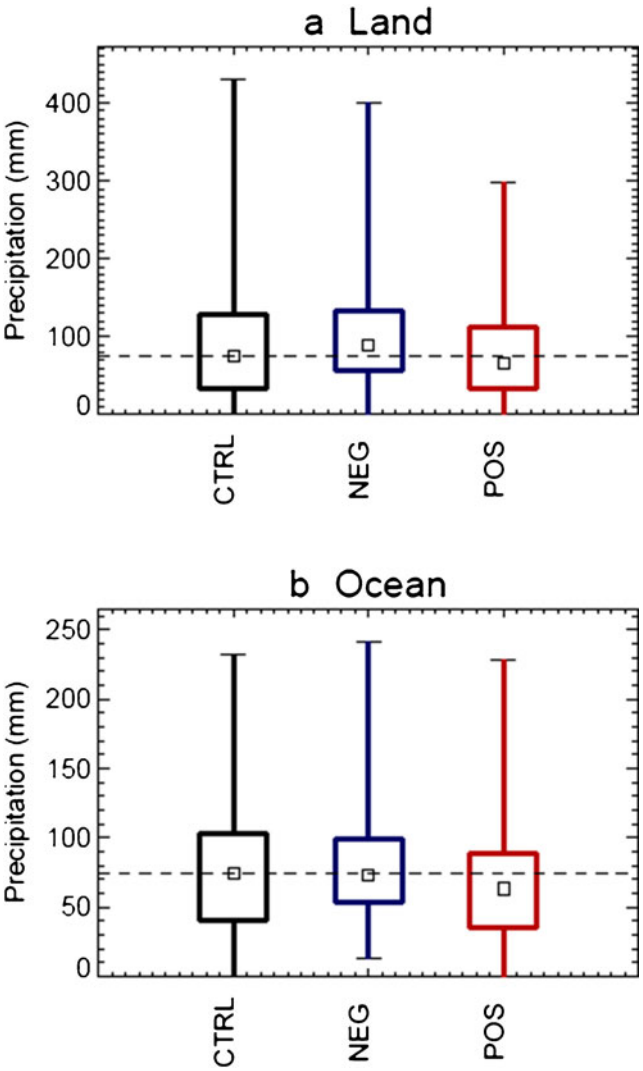

Fig. 10 Box plot of accumulated precipitation from December 11 to 17 over **a** land and **b** the ocean. The box plot is built on the spatial distribution of accumulated precipitation taking all ensemble members into account. The *whiskers* are defined as 1.5 times the interquartile range. The control ensemble is shown in *black*, NEG ensemble is shown in *blue*, and POS ensemble is shown in *red*. The *dashed line* represents the median for the control ensemble as a baseline comparison. The statistical significance for the difference in the median, upper, and lower quartiles are shown in Table 2

by the NEG experiments showed an increase in the 25th percentile and in the median (Fig. 10a, Table 2). On the other hand, POS experiments showed a decrease in the median and in the 25th and 75th percentiles (Fig. 10a, Table 2). In addition, the overall range of the spatial variability of the accumulated precipitation showed a small reduction in the NEG experiments and a considerable reduction in the POS experiments (Fig. 10a). These results are in agreement with the observational analyses, which showed that SAD-negative phase is associated with increased precipitation over eastern South America and SAD-positive phase is related to decreased precipitation in that region (Bombardi et al. 2013).

Over the ocean, the POS experiments also indicated a reduction in the median, 75th, and 95th percentiles of the accumulated precipitation distribution (Fig. 10b; Table 2). The observational analysis also revealed a decrease in precipitation over the oceanic portion of the SACZ near the coast during the positive SAD phase. However, regarding the spatial distribution of accumulated precipitation, the NEG experiments did not show statistically significant differences in the median for the oceanic SACZ. Although no clear change is verified for the median accumulated precipitation in the NEG experiments, there was a decrease in the 75th percentile and an increase in the 25th and 95th percentiles of the precipitation distribution (Fig. 10b; Table 2).

The daily precipitation RMSE and BIAS between the perturbed and the control experiments were calculated spatially over land and the oceanic portion of the SACZ (Fig. 11). Daily precipitation ensemble means were calculated for each experiment prior to the calculation of RMSE and BIAS. Daily

Table 2 Differences in the percentiles of the distributions of accumulated precipitation associated with the SACZ over land and ocean (see Fig. 10) between the perturbed experiments and the control experiment

LAND percentile	NEG-CTRL (mm)	POS-CTRL (mm)
25 %	23.9[a]	1.0
50 %	13.6 [a]	-9.3 [a]
75 %	3.8	-17.1 [a]
95 %	−9.1	−44.9 [a]
OCEAN percentile		
25 %	13.1 [a]	−4.2
50 %	−1.4	−10.9 [a]
75 %	−4.1 [a]	−14.8 [a]
95 %	7.6	−18.0 [a]

[a] Differences that are statistically significant at 5 % level according to the sign test for difference in locations (Anderson and Finn 1996)

variance was larger in the NEG experiment than in the POS experiment over both land (Fig. 11a) and the ocean (Fig. 11b). In addition, the largest deviations in the NEG experiment over land occurred just before the formation and during the first days of the active period of the cyclone, between December 13 and 16 (Fig. 11a). Over the ocean, the largest deviations in the NEG experiment occurred during the active period of the cyclone, between December 14 and 17 (Fig. 11b). The NEG experiments simulated more precipitation than the control experiment for most of the days over both land (Fig. 11c) and the ocean (Fig. 11d). On the other hand, the POS experiments simulated less precipitation than the control experiments for most of the days over both land (Fig. 11c) and the ocean (Fig. 11d). However, the NEG experiments showed an inversion in the BIAS sign on December 16 and 17 over the ocean (Fig. 11d) that could partially explain the low statistical significance in the calculations of the differences in the accumulated precipitation distribution (Fig. 10b; Table 2).

Figure 12 shows the differences between NEG and the control experiments and between POS and the control experiments. On day 11, the NEG experiments showed an anomalous cyclonic circulation over central South America (Fig. 12a). This anomalous circulation indicates the weakening of the low level jet east of the Andes, which is consistent with the intensification of convection in the SACZ (Liebmann et al. 2004). In contrast, the POS experiment showed an anomalous anticyclonic circulation over western Brazil, which in turn was associated with the intensification of the northerly winds east of the Andes (Fig. 12b). In addition, it is noticeable that the cyclonic (anticyclonic) anomalous circulations over tropical South America in the NEG (POS) experiments caused the westerly wind anomalies to shift equatorward (poleward) comparatively to the control. These features were also consistent with the equatorward shift of convection in the NEG experiments and the suppression of convection in the POS experiment relative to the control (see Fig. 9).

On December 12, the NEG experiment indicated an increase in the westerly flow in a narrow band extending from

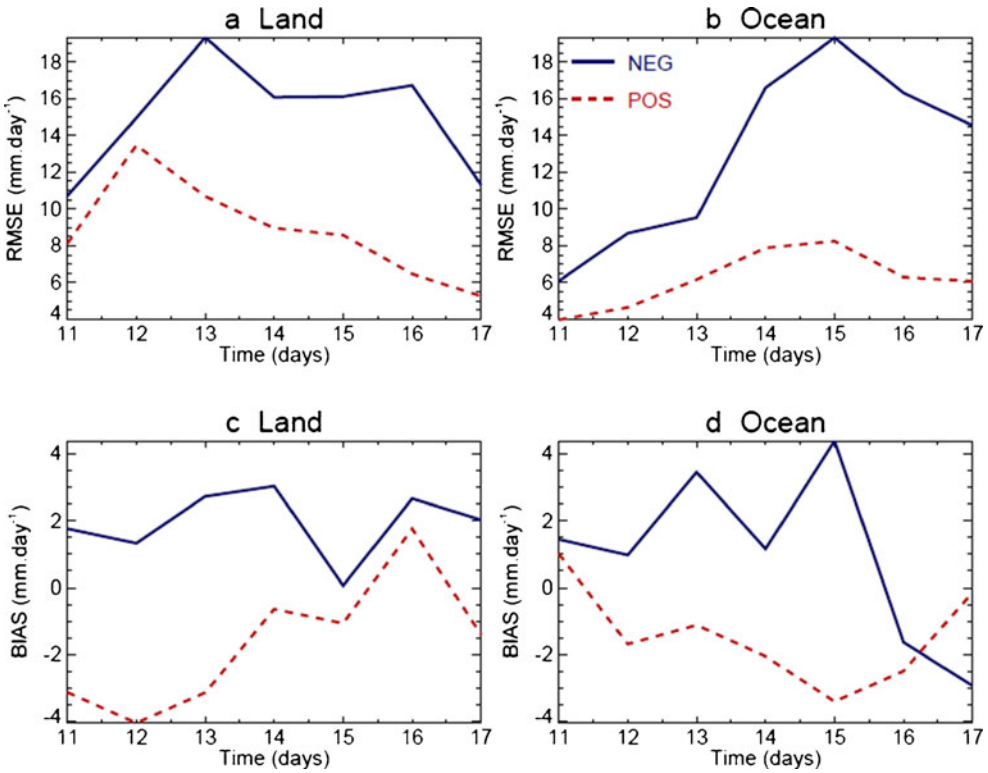

Fig. 11 Daily precipitation RMSE between the ensembles mean of the perturbed experiments and the control experiment for **a** land and **b** the ocean. Daily precipitation BIAS between the ensemble mean of the perturbed experiments and the control experiments over **c** land and **d** the ocean. *Solid lines* refer to NEG and *dashed lines* to POS experiments

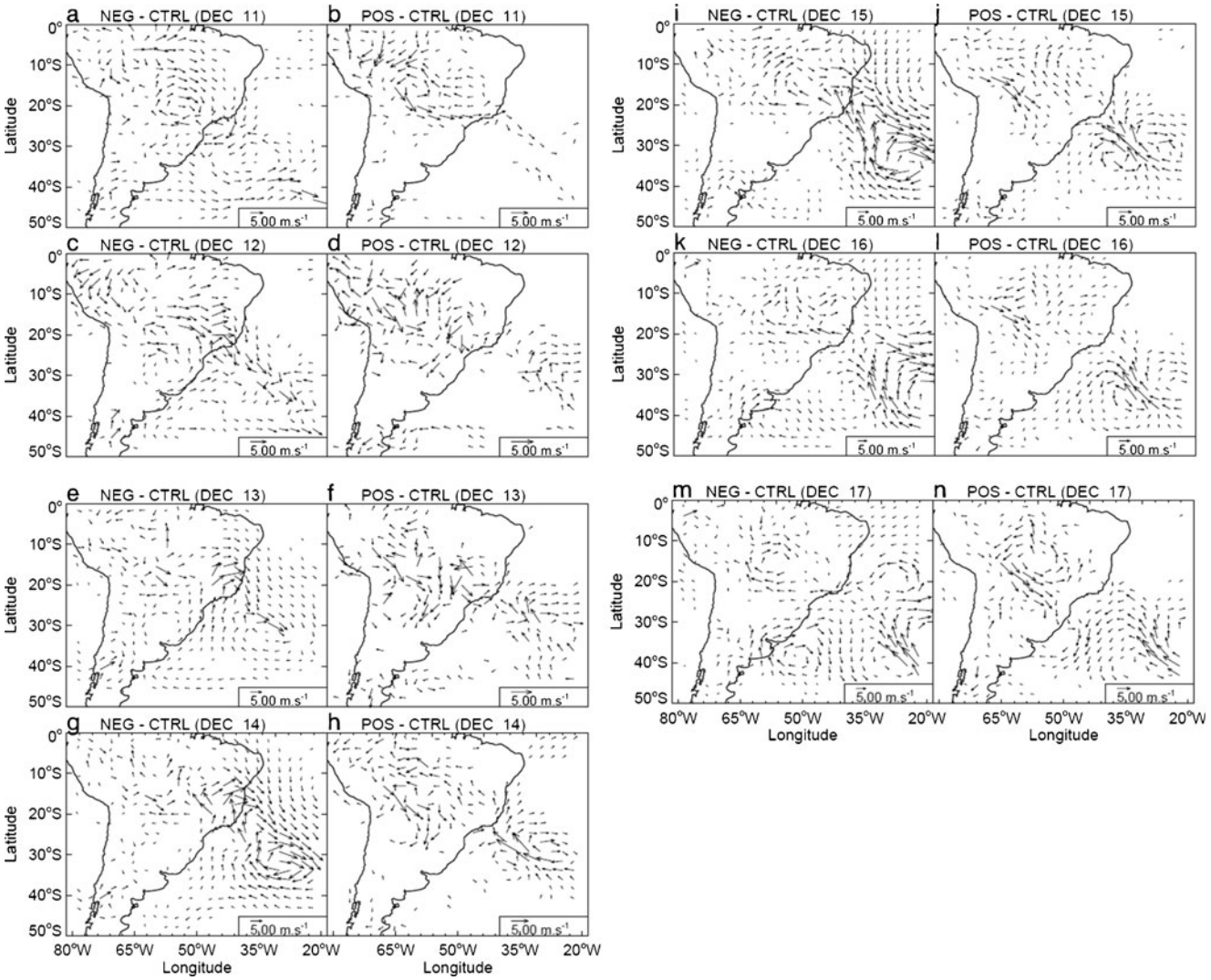

Fig. 12 Daily evolution of the difference in the ensemble mean wind at 850 hPa between perturbed experiments and the control experiment. Differences for the NEG experiment are in the *left* and for the POS experiment are in the *right*. Vectors are displayed only where the differences are greater than 1.0 m s^{-1} and statistically significant at 5 % level (for the zonal or the meridional component of the wind) according to a z-test with 9° of freedom (Anderson and Finn 1996) (continues)

the Amazon toward the subtropical South Atlantic, which characterized the warm conveyor belt (Browning 1986; Hallak and Silva Dias 2000) and enhanced convection commonly associated with the SACZ (Carvalho LM et al. 2004; Jones and Carvalho 2002; Jorgetti et al. 2013; Rickenbach 2002) (Fig. 12c). Furthermore, the westerly wind anomalies were important for the transport of moist static energy from the Amazon with implications for the intensified convection in the SACZ (Chou and Neelin 2001; Neelin and Held 1987). These features were not evident for the POS experiment, which is consistent with the suppressed convection in the SACZ region.

On December 13 and 14, the anomalous westerly flow persisted and moved equatorward in the NEG experiment as the cyclone over subtropical Atlantic propagates eastward (Fig. 12e, g). In contrast, on December 13 and 14 the POS experiment showed easterly wind anomalies collocated with the modeled SACZ. The easterlies anomalies implied in a relatively more stable air (Neelin and Held 1987) and weaker SACZ relative to the control (Fig. 12f, h).

The cyclone over the Subtropical Western Atlantic that was well developed on December 14 in the NEG experiment intensified and moved southeastward from December 15–17 (Fig. 12g, i, k, m). In contrast, the easterly anomalies over the Subtropical South Atlantic persisted on December 15–18 in the POS experiment, clearly indicating the persistence of relatively unfavorable dynamic and thermodynamic conditions for enhanced SACZ over the continent and the ocean (Fig. 12h, j, l, n). The warm conveyor belt supporting convection in the SACZ in the NEG experiment weakened on

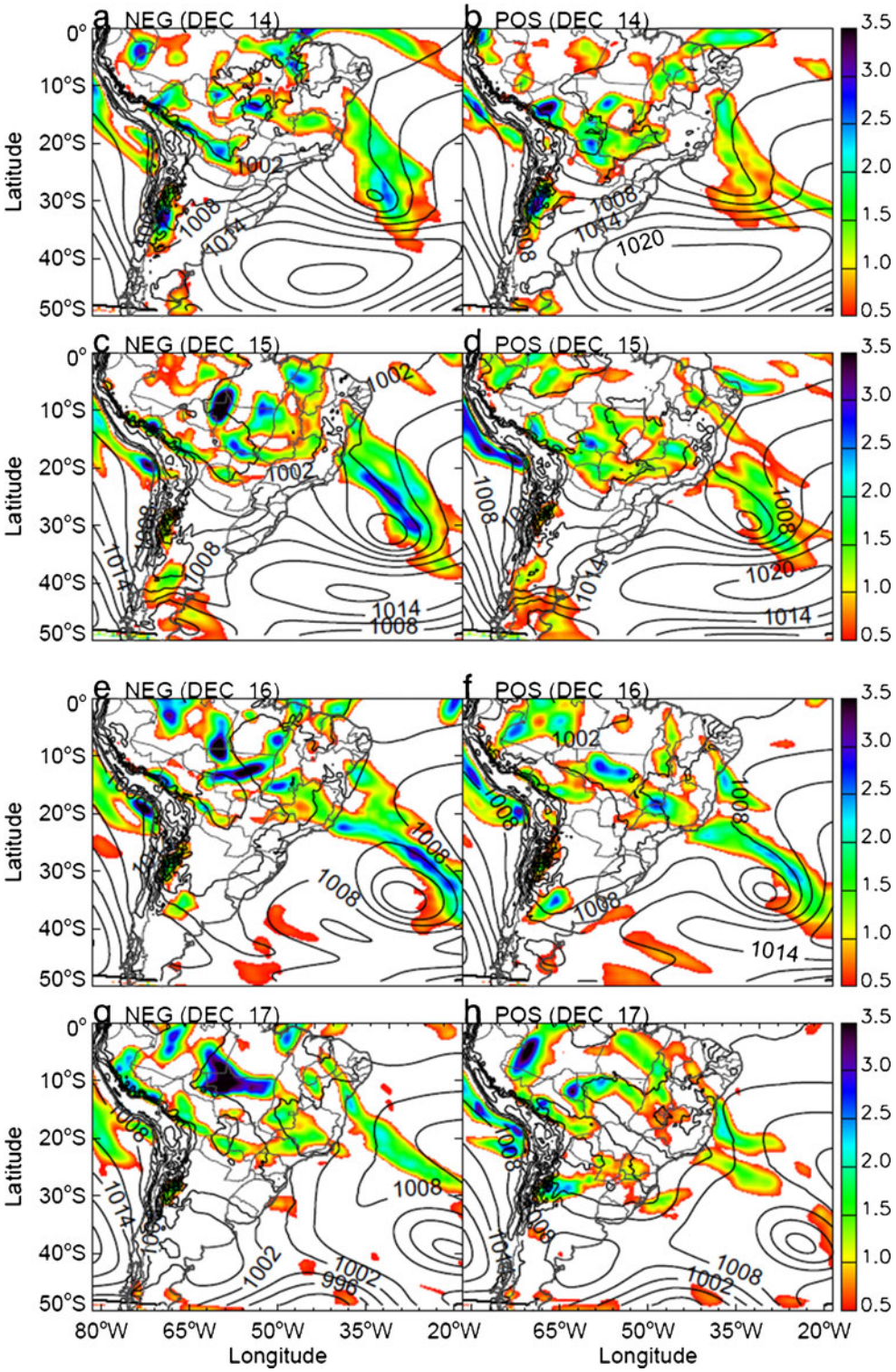

Fig. 13 Evolution of daily SLP (contour) and 200 hPa wind divergence (*shaded*) from December 14 to 17 for the mean NEG ensemble (*left*) and the mean POS ensemble (*right*). Contour interval equal 3 hPa. Wind divergence unit equal 10-5 s^{-1}. Only positive wind divergence is displayed

December 17, which characterized the end of the cycle of intense precipitation associated with the system (Fig. 12n).

Figure 13 shows the evolution of the daily mean ensemble SLP and wind divergence at 200 hPa during the period when the cyclone was active over the Atlantic Ocean. The low pressure system was much stronger in NEG simulations (Fig. 13a, c, e, g) than in POS simulations (Fig. 13b, d, f, h). In addition, the upper level wind divergence giving support to the cyclone was stronger in the NEG simulations than in the POS simulations (Figs. 13 and 14). These results indicated that, during SAD-negative events, the upper-level divergence strengthened the low pressure system at the surface. The

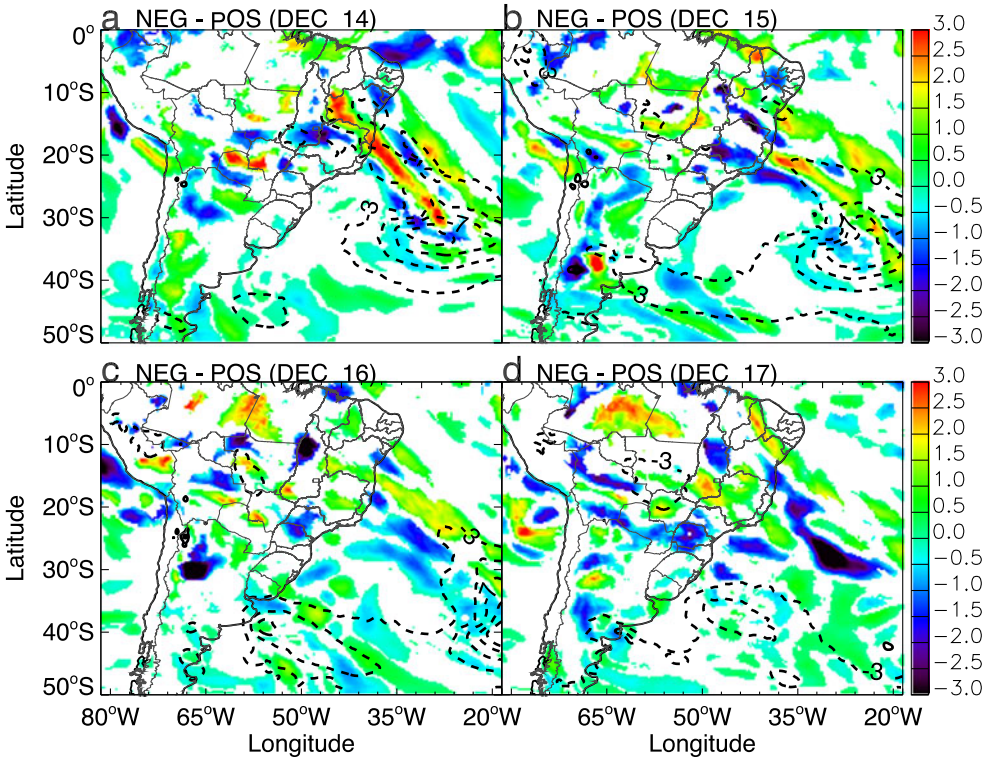

Fig. 14 Difference in the ensemble median of 200 hPa wind divergence (*shaded*) and SLP (contour) between NEG and POS from December 14 to 17. Only positive values of divergence were taken into account. *Shading* indicates ensemble median differences that are statistically significant at 5 % level according to the sign test. Contours indicate ensemble median differences that are statistically significant at 5 % level according to the sign test and with absolute value greater or equal to 3 hPa. Contour interval equals 3 hPa. *Dashed lines* represent negative values

strengthening of the low pressure system increased the low level westerly winds and transport of moist static energy from the Amazon along the southwestern periphery of the subtropical high. These dynamical conditions intensified convection and precipitation in the SACZ.

In conclusion, these experiments demonstrated that the realistic simulations of the position of the SACZ and the patterns of precipitation over coastal areas in South America are to a large extent determined by the anomalous atmospheric driving fields associated with SAD events. The position of the low and high level jets and the upper level divergence, the evolution and displacement of cyclones and anticyclones ultimately determine the support for convection in the SACZ region. More importantly, even though it is expected that realistic atmospheric forcing results in realistic simulations of convective activity, we showed that the idealized sensitivity experiments with SST resulted in patters of precipitation that are contrary to observations. In other words, the moisture and heat fluxes (sensible and latent heat fluxes) resulting from the observed pattern of SST anomalies during SAD somewhat opposes to the forcing caused by the atmosphere.

Nevertheless, both driving fields and SST sensitivity experiments showed that the main impact of SAD is associated with changes in the location and strength of the cyclone at the surface over subtropical South Atlantic. It is important to keep in mind that this study did not address ocean–atmosphere coupling. In reality, ocean–atmosphere feedbacks would play an important role for the coupled mechanisms linking the South Atlantic Ocean to the South American climate. Moreover, experiments forced with prescribed SST cannot fully represent the ocean-atmosphere interactions and therefore do not correctly represent the lower boundary conditions (Bretherton and Battisti 2000; Sutton and Mathieu 2002). For example, Sutton and Mathieu (2002) showed that the influence of the extratropical ocean on climate is not manifested primarily in an SST signature. A better approach would be to couple the atmospheric model to an ocean mixed layer model with a prescribed ocean heat convergence (e.g., Sutton and Mathieu 2002). Such approach would give a better understanding on the role of the ocean and the development of the pattern of SST due to a more realistic representation of ocean heat convergence and surface fluxes.

6 Conclusions

The present study explored numerical simulations of a SACZ event that occurred under neutral ENSO and neutral SAD conditions. We performed experiments forced with SAD SST conditions and experiments forced with SAD atmospheric conditions. Our results confirm previous observational studies and show that SAD plays a significant role in organizing the SACZ by influencing the position and movement of extratropical cyclones. However, the numerical experiments suggest that, during ENSO neutral conditions, the SACZ

precipitation variability associated with SAD is largely dependent on the atmospheric variability rather than the underlying SST.

The BRAMS 4.2 model was able to represent the spatial pattern of precipitation and circulation during the SACZ event of December 2005. However, the model underestimates the daily total precipitation over the oceanic portion of the SACZ. Experiments forced with prescribed SST anomalies showed that the SACZ precipitation is not significantly influenced by the Atlantic SST. Nonetheless, the SST sensitivity experiments showed that the Atlantic SST is related to the position of the cyclone associated to the SACZ. Positive SAD SST anomaly forcing (warm tropical SST anomalies) shifts the cyclone and the SACZ northward. On the other hand, negative SAD SST anomaly forcing (cold tropical SST anomalies) moves the cyclone and the SACZ southward. However, the atmospheric response and precipitation patterns obtained with the SST forcing experiments opposed to the observational results.

On the other hand, experiments forced with prescribed driving fields anomalies showed that the atmospheric component of SAD also impacts the characteristics of the cyclone over the South Atlantic Ocean and plays a key role for the positioning of the SACZ. SAD-negative anomalies favor the intensification of the westerly low-level wind anomalies on the equatorward flank of the SACZ as well as the intensification of the upper-level jet stream. Therefore, the atmosphere provides the low-level and upper-level support for the intensification of the cyclone at surface and for the increase in precipitation over the coastal areas in association with the SACZ. In contrast, SAD-positive anomalies generate an opposite response in the atmosphere.

It is worth noting that the SACZ is a transient system strongly influenced by intraseasonal variability (Carvalho LM et al. 2004; Liebmann et al. 1999). Although SAD temporal variability is dominated by decadal timescales, there is also significant variability on intraseasonal timescales, and we showed evidence that these variations play a significant role for the characteristics of the SACZ (Bombardi et al. 2013).

Acknowledgment We thank the anonymous reviewers for their valuable comments and suggestions for the improvement of this manuscript. We thank the support of NOAA Climate Program Office (NA07OAR4310211 and NA10OAR4310170). This research was conducted under the CGIAR Research Program on Climate Change, Agriculture and Food Security (CCAFS), sub-contract with the International Potato Center (SB120184). L. Carvalho thanks FAPESP (2008/58101-9) and CNPq [555768/2010-4]. We thank NASA for making available the MERRA reanalysis, NOAA for making available the SST data, and ANA for making available the precipitation station data. We also thank Dr. Brant Liebmann and Dr. David Allured for providing the precipitation station data. R. Bombardi thanks Dr. Saulo Freitas and Dr. Edmilson Dias de Freitas for their help with the BRAMS model.

References

Almeida RAF, Nobre P, Haarsma RJ, Campos EJD (2007) Negative ocean–atmosphere feedback in the South Atlantic Convergence Zone. Geophys Res Lett 34, L18809. doi:10.1029/2007GL030401

Alonso MF, Longo KM, Freitas SR et al (2010) An urban emissions inventory for South America and its application in numerical modeling of atmospheric chemical composition at local and regional scales. Atmos Environ 44:5072–5083. doi:10.1016/j.atmosenv.2010.09.013

Anderson TW, Finn JD (1996) The new statistical analysis of data. Springer-Verlag, New York, p 712

Arakawa A, Schubert WH (1974) Interaction of a cumulus cloud ensemble with the large-scale environment, part I. J Atmos Sci 31:674–701. doi:10.1175/1520-0469(1974)031<0674:IOACCE>2.0.CO;2

Barreiro M (2009) Influence of ENSO and the South Atlantic Ocean on climate predictability over Southeastern South America. Clim Dyn 35:1493–1508. doi:10.1007/s00382-009-0666-9

Barreiro M, Chang P, Saravanan R (2002) Variability of the South Atlantic Convergence Zone simulated by an atmospheric general circulation model. J Climate 15:745–763. doi:10.1175/1520-0442(2002)015<0745:VOTSAC>2.0.CO;2

Barreiro M, Chang P, Saravanan R (2005) Simulated precipitation response to SST forcing and potential predictability in the region of the South Atlantic convergence zone. Clim Dyn 24:105–114. doi:10.1007/s00382-004-0487-9

Bombardi RJ, Carvalho LMV (2011) The South Atlantic dipole and variations in the characteristics of the South American Monsoon in the WCRP-CMIP3 multi-model simulations. Clim Dyn 36:2091–2102. doi:10.1007/s00382-010-0836-9

Bombardi RJ, Carvalho LMV, Jones C, Reboita MS (2013) Precipitation over eastern South America and the South Atlantic Sea surface temperature during neutral ENSO periods. Clim Dyn. doi:10.1007/s00382-013-1832-7

Bookhagen B, Strecker MR (2010) Modern Andean rainfall variation during ENSO cycles and its impact on the Amazon drainage basin. Diversity. In: Hoorn C, Wesselingh FP (eds) Amaz. Landsc. Species Evol. A look into past. Wiley-Blackwell Publishing Ltd, Oxford, UK, pp 223–241

Bretherton CS, Battisti DS (2000) An interpretation of the results from atmospheric general circulation models forced by the time history of the observed sea surface temperature distribution. Geophys Res Lett 27:767–770. doi:10.1029/1999GL010910

Browning KA (1986) Conceptual models of precipitation systems. Weather Forecast 1:23–41. doi:10.1175/1520-0434(1986)001<0023:CMOPS>2.0.CO;2

Carvalho LMV, Jones C, Silva Dias MAF (2002a) Intraseasonal large-scale circulations and mesoscale convective activity in tropical South America during the TRMM-LBA campaign. J Geophys Res 107:8042. doi:10.1029/2001JD000745

Carvalho LM V, Jones C, Liebmann B (2002b) Extreme precipitation events in Southeastern South America and large-scale convective patterns in the South Atlantic Convergence Zone. J Climate 15:2377–2394. doi:10.1175/1520-0442(2002)015<2377:EPEISS>2.0.CO;2

Carvalho LMV, Jones C, Liebmann B (2004) The South Atlantic Convergence Zone: intensity, form, persistence, and relationships with intraseasonal to interannual activity and extreme rainfall. J Climate 17:88–108. doi:10.1175/1520-0442(2004)017<0088:TSACZI>2.0.CO;2

Carvalho LMV, Jones C, Posadas AND et al (2012) Precipitation characteristics of the South American monsoon system derived from multiple datasets. J Climate 25:4600–4620. doi:10.1175/JCLI-D-11-00335.1

Chaves RR, Nobre P (2004) Interactions between sea surface temperature over the South Atlantic Ocean and the South Atlantic Convergence Zone. Geophys Res Lett 31, L03204. doi:10.1029/2003GL018647

Chen C, Cotton WR (1983) A one-dimensional simulation of the stratocumulus-capped mixed layer. Boundary-Layer Meteorol 25: 289–321. doi:10.1007/BF00119541

Chen M, Shi W, Xie P et al (2008) Assessing objective techniques for gauge-based analyses of global daily precipitation. J Geophys Res 113, D04110. doi:10.1029/2007JD009132

Chou C, Neelin JD (2001) Mechanisms limiting the southward extent of the South American Summer Monsoon. Geophys Res Lett 28:2433–2436. doi:10.1029/2000GL012138

Cotton WR, Pielke RA Sr, Walko RL et al (2003) RAMS 2001: current status and future directions. Meteorol Atmos Phys 82:5–29. doi:10.1007/s00703-001-0584-9

Cuadra SV, Da Rocha RP (2007) Sensitivity of regional climatic simulation over Southeastern South America to SST specification during austral summer. Int J Climatol 27:793–804. doi:10.1002/joc.1431

de O Cardoso A, Silva Dias PL (2004) Atlantic and Pacific variability and temperature during the winter season in Sao Paulo City. Rev Bras Meteorol 19:113–122

Freitas SR, Longo KM, Silva Dias MAF et al (2009) The coupled aerosol and tracer transport model to the Brazilian developments on the Regional Atmospheric Modeling System (CATT-BRAMS)—part 1: model description and evaluation. Atmos Chem Phys 9:2843–2861. doi:10.5194/acp-9-2843-2009

Gevaerd R, Freitas S (2006) Operational soil moisture estimate for initialization of numerical weather forecast models—part I: model description and validation. Rev Bras Meteorol 21:1–15

Giorgi F, Bi X (2000) A study of internal variability of a regional climate model. J Geophys Res 105:29503–29521. doi:10.1029/2000JD900269

Grell GA (1993) Prognostic evaluation of assumptions used by cumulus parameterizations. Mon Weather Rev 121:764–787. doi:10.1175/1520-0493(1993)121<0764:PEOAUB>2.0.CO;2

Haarsma RJ (2003) Atmospheric response to South Atlantic SST dipole. Geophys Res Lett 30:1864. doi:10.1029/2003GL017829

Haarsma RJ, Campos EJD, Hazeleger W et al (2005) Dominant modes of variability in the South Atlantic: a study with a hierarchy of ocean–atmosphere models. J Climate 18:1719–1735. doi:10.1175/JCLI3370.1

Hallak R, Silva Dias MAF (2000) 1827 ESTUDO DIAGNÓSTICO DE UM VÓRTICE DE AR FRIO—PARTE I: ASPECTOS DE GRANDE ESCALA. XI Congr. Bras. Meteorol. pp 1682–1691

Herdies DL (2002) Moisture budget of the bimodal pattern of the summer circulation over South America. J Geophys Res 107:8075. doi:10.1029/2001JD000997

Higgins RW, Shi W, Yarosh E, Joyce R (2000) Improved United States precipitation quality control system and analysis. NCEP/Climate Predict Cent atlas no 7:40

Huffman GJ, Bolvin DT, Nelkin EJ et al (2007) The TRMM Multisatellite Precipitation Analysis (TMPA): quasi-global, multiyear, combined-sensor precipitation estimates at fine scales. J Hydrometeorol 8:38–55. doi:10.1175/JHM560.1

Jones C, Carvalho LMV (2002) Active and break phases in the South American Monsoon System. J Climate 15:905–914. doi:10.1175/1520-0442(2002)015<0905:AABPIT>2.0.CO;2

Jorgetti T (2008) The South Atlantic Convergence Zone and Oceanic Processes in the Atlantic and the Pacific. Dissertation, University of Sao Paulo. 169. Available at University of Sao Paulo

Jorgetti T, SIlva Dias PL, Freitas ED (2013) The relationship between South Atlantic SST and SACZ intensity and positioning. Theor. Appl. Climatol

Joyce RJ, Janowiak JE, Arkin PA, Xie P (2004) CMORPH: a method that produces global precipitation estimates from passive microwave and infrared data at high spatial and temporal resolution. J Hydrometeorol 5:487–503. doi:10.1175/1525-7541(2004)005<0487:CAMTPG>2.0.CO;2

Kodama Y (1992) Large-scale common features of subtropical precipitation zones (the baiu Frontal Zone, the SPCZ, and the SACZ) part I: characteristics of subtropical frontal zones. J Meteorol Soc Japan 70: 813–835

Kodama Y (1993) Large-scale common features of subtropical precipitation zones (the baiu Frontal Zone, the SPCZ, and the SACZ) part II: conditions of the circulations for generating the STCZs. J Meteorol Soc Japan 71:581–610

Kodama Y-M (1999) Roles of the atmospheric heat sources in maintaining the subtropical convergence zones – an aquaplanet GCM study. J Atmos Sci 56:4032–4049

Kummerow C, Barnes W, Kozu T et al (1998) The Tropical Rainfall Measuring Mission (TRMM) sensor package. J Atmos Oceanic Tech 15:809–817. doi:10.1175/1520-0426(1998)015<0809:TTRMMT>2.0.CO;2

Kummerow C, Simpson J, Thiele O et al (2000) The status of the Tropical Rainfall Measuring Mission (TRMM) after two years in orbit. J Appl Meteorol 39:1965–1982. doi:10.1175/1520-0450(2001)040<1965:TSOTTR>2.0.CO;2

Liebmann B, Kiladis GN, Marengo J et al (1999) Submonthly convective variability over South America and the South Atlantic Convergence Zone. J Climate 12:1877–1891. doi:10.1175/1520-0442(1999)012<1877:SCVOSA>2.0.CO;2

Liebmann B, Jones C, Carvalho LMV (2001) Interannual variability of daily extreme precipitation events in the state of São Paulo, Brazil. J Climate 14:208–218. doi:10.1175/1520-0442(2001)014<0208:IVODEP>2.0.CO;2

Liebmann B, Kiladis GN, Vera CS et al (2004) Subseasonal variations of Rainfall in South America in the vicinity of the low-level jet east of the Andes and comparison to those in the South Atlantic Convergence Zone. J Climate 17:3829–3842. doi:10.1175/1520-0442(2004)017<3829:SVORIS>2.0.CO;2

Longo KM, Freitas SR, Andreae MO et al (2010) The coupled aerosol and tracer transport model to the Brazilian developments on the Regional Atmospheric Modeling System (CATT-BRAMS)—part 2: model sensitivity to the biomass burning inventories. Atmos Chem Phys 10:5785–5795. doi:10.5194/acp-10-5785-2010

Marsal D (1987) Statistics for geoscientists, 1st ed. 176

Morioka Y, Tozuka T, Yamagata T (2011) On the growth and decay of the subtropical dipole mode in the South Atlantic. J Climate 24:5538–5554. doi:10.1175/2011JCLI4010.1

Moura AD, Shukla J (1981) On the dynamics of droughts in Northeast Brazil: observations, theory and numerical experiments with a general circulation model. J Atmos Sci 38:2653–2675. doi:10.1175/1520-0469(1981)038<2653:OTDODI>2.0.CO;2

Muza MN, Carvalho LMV, Jones C, Liebmann B (2009) Intraseasonal and interannual variability of extreme dry and wet events over southeastern South America and the subtropical Atlantic during austral summer. J Climate 22:1682–1699. doi:10.1175/2008JCLI2257.1

Neelin JD, Held IM (1987) Modeling tropical convergence based on the moist static energy budget. Mon Weather Rev 115:3–12. doi:10.1175/1520-0493(1987)115<0003:MTCBOT>2.0.CO;2

Nnamchi HC, Li J, Anyadike RNC (2011) Does a dipole mode really exist in the South Atlantic Ocean? J Geophys Res 116, D15104. doi:10.1029/2010JD015579

Pielke RA, Cotton WR, Walko RL et al (1992) A comprehensive meteorological modeling system—RAMS. Meteorol Atmos Phys 49:69–91. doi:10.1007/BF01025401

Reboita MS (2008) Extratropical cyclones over the South Atlantic Ocean: climatic simulation and sensibility experiments. Dissertation, University of Sao Paulo. 294. Available at University of Sao Paulo

Reynolds RW, Rayner NA, Smith TM et al (2002) An improved in situ and satellite SST analysis for climate. J Climate 15:1609–1625. doi:10.1175/1520-0442(2002)015<1609:AIISAS>2.0.CO;2

Reynolds RW, Smith TM, Liu C et al (2007) Daily high-resolution-blended analyses for sea surface temperature. J Climate 20:5473–5496. doi:10.1175/2007JCLI1824.1

Rickenbach TM (2002) Modulation of convection in the southwestern Amazon basin by extratropical stationary fronts. J Geophys Res 107: 8040. doi:10.1029/2000JD000263

Rienecker MM, Suarez MJ, Gelaro R et al (2011) MERRA: NASA's modern-era retrospective analysis for research and applications. J Climate 24:3624–3648. doi:10.1175/JCLI-D-11-00015.1

Robertson AW, Mechoso CR (2000) Interannual and interdecadal variability of the South Atlantic Convergence Zone. Mon Weather Rev 128:2947–2957. doi:10.1175/1520-0493(2000)128<2947:IAIVOT>2.0.CO;2

Robertson AW, Farrara JD, Mechoso CR (2003) Simulations of the atmospheric response to South Atlantic Sea Surface Temperature anomalies. J Climate 16:2540–2551. doi:10.1175/1520-0442(2003)016<2540:SOTART>2.0.CO;2

Rodwell MJ, Hoskins BJ (2001) Subtropical anticyclones and summer monsoons. J Climate 14:3192–3211

Santos AF, Freitas SR, de Mattos JGZ et al (2013) Using the Firefly optimization method to weight an ensemble of rainfall forecasts from the Brazilian developments on the Regional Atmospheric Modeling System (BRAMS). Adv Geosci 35:123–136. doi:10.5194/adgeo-35-123-2013

Sterl A, Hazeleger W (2003) Coupled variability and air–sea interaction in the South Atlantic Ocean. Clim Dyn 21:559–571. doi:10.1007/s00382-003-0348-y

Sutton R, Mathieu P-P (2002) Response of the atmosphere–ocean mixed-layer system to anomalous ocean heat-flux convergence. Q J Roy Meteorol Soc 128:1259–1275. doi:10.1256/003590002320373283

Taschetto AS, Wainer I (2008) The impact of the subtropical South Atlantic SST on South American precipitation. Ann Geophys 26: 3457–3476. doi:10.5194/angeo-26-3457-2008

Tomaziello ACN, Gandu AW (2013) Impacto da temperatura da superfície do mar na simulação da Zona de Convergência do Atlântico Sul. Rev Bras Meteorol 28:291–304. doi:10.1590/S0102-77862013000300006

Uvo CB, Repelli CA, Zebiak SE, Kushnir Y (1998) The relationships between tropical Pacific and Atlantic SST and Northeast Brazil monthly precipitation. J Climate 11:551–562. doi:10.1175/1520-0442(1998)011<0551:TRBTPA>2.0.CO;2

Venegas SA, Mysak LA, Straub DN (1997) Atmosphere–ocean coupled variability in the South Atlantic. J Climate 10:2904–2920. doi:10.1175/1520-0442(1997)010<2904:AOCVIT>2.0.CO;2

Vera C, Higgins W, Amador J et al (2006) Toward a unified view of the American monsoon systems. J Climate 19:4977–5000. doi:10.1175/JCLI3896.1

Walko RL, Band LE, Baron J et al (2000) Coupled atmosphere–biophysics–hydrology models for environmental modeling. J Appl Meteorol 39:931–944. doi:10.1175/1520-0450(2000)039<0931:CABHMF>2.0.CO;2

Weaver CP (2002) Sensitivity of simulated mesoscale atmospheric circulations resulting from landscape heterogeneity to aspects of model configuration. J Geophys Res 107:8041. doi:10.1029/2001JD000376

Zhou J, Lau K-M (1998) Does a monsoon climate exist over South America? J Climate 11:1020–1040. doi:10.1175/1520-0442(1998)011<1020:DAMCEO>2.0.CO;2